

## Travelling-Wave Similarity Solutions for an Unsteady Shear-Stress-Driven Dry Patch in a Flowing Film

(Penyelesaian Keserupaan Gelombang Menjalar bagi Aliran Tak Mantap di Sekitar Tompokan Kering yang Didorong oleh Tegasan Ricih)

YAZARIAH M. YATIM\*, BRIAN R. DUFFY & STEPHEN K. WILSON

### ABSTRACT

*We investigate unsteady flow of a thin film of Newtonian fluid around a symmetric slender dry patch moving with constant velocity on an inclined planar substrate, the flow being driven by a prescribed constant shear stress at the free surface of the film (which would be of uniform thickness in the absence of the dry patch). We obtain a novel unsteady travelling-wave similarity solution which predicts that the dry patch has a parabolic shape and that the film thickness increases monotonically away from the dry patch.*

*Keywords: Dry patch; similarity solution; thin-film flow; travelling-wave*

### ABSTRAK

*Kami mengkaji aliran tak mantap filem nipis bendalir Newtonian di sekitar tompokan kering simetri yang bergerak dengan halaju yang malar di atas substrat yang condong. Aliran tersebut didorong oleh tegasan ricih yang malar pada permukaan bebas filem itu (yang mempunyai ketebalan yang seragam sekiranya tompokan kering tidak wujud). Kami memperoleh penyelesaian keserupaan gelombang menjalar bagi tompokan kering yang menunjukkan tompokan kering tersebut berbentuk parabola dan ketebalan filem menjauhi tompokan kering didapati bertambah secara monotonik.*

*Kata kunci: Aliran filem nipis; gelombang menjalar; penyelesaian keserupaan; tompokan kering*

### INTRODUCTION

A dry patch can occur in a fluid film for many reasons, including there being insufficient fluid to wet the substrate, a high temperature of the substrate which causes the fluid to dry out, the presence of air bubbles within the film, inhomogeneities in the substrate or the presence of surfactant in the fluid. A common example of dry patch formation is when a thin film of fluid runs down an inclined plane, forming fingers (rivulets) with dry patches in-between. This problem is of considerable practical interest, especially in industrial contexts such as in heat exchangers and coating processes. In a heat-transfer device, the presence of dry patches must generally be avoided because it may reduce the efficiency or may result in overheating or corrosion of the dry area in the device. In coating processes the formation of dry patches is also clearly undesirable and therefore it is crucial to understand when a layer of fluid will leave a hole on the substrate and whether the holes that exist will persist or will close up during the coating process.

Pioneering work on a dry patch in a flowing fluid film driven either by gravity or by a prescribed surface shear stress due to an external air flow was performed by Hartley and Murgatroyd (1964) and extended by Murgatroyd (1965). Wilson et al. (2001) obtained two steady similarity solutions for a flow around a non-uniform

slender dry patch in a thin film draining under gravity on an inclined plane, namely one for the case of weak surface tension and one for the case of strong surface tension. Early experiments on the shape and structure of a dry patch in a fluid film draining under gravity down the outside of a vertical circular cylinder were performed by Ponter et al. (1967), and over the last decade or so the shape and structure of a dry patch in a fluid film draining under gravity down an inclined plane has been extensively studied both experimentally and theoretically by Limat and his collaborators (Podgorski et al. 1999, 2001; Rio et al. 2004; Rio & Limat 2006; Sébilleau et al. 2009).

Since it seems to concern numerous practical situations, understanding the appearance of dry patches and their evolution is important. While the mechanism of dry patch formation is practically understood, the problem of investigating the unsteady flow of Newtonian fluid around a dry patch has not yet been solved satisfactorily. Motivated by this, we use the lubrication approximation to analyse three-dimensional unsteady flow of a thin film of Newtonian fluid around a symmetric slender moving dry patch on an inclined planar substrate, the flow being driven by a prescribed constant shear stress at the free surface. The appropriate governing equations are analysed numerically and asymptotically in appropriate asymptotic limits.

PROBLEM FORMULATION

Consider a thin film of Newtonian fluid with constant density  $\rho$  and constant viscosity  $\mu$  on a planar substrate inclined at an angle  $\alpha$  ( $0 < \alpha < \pi$ ) to the horizontal, subject to gravitational acceleration  $g$  and a prescribed stress  $\tau$  ( $> 0$ ) on its free surface acting down the substrate. We shall be concerned with unsteady flow of such a film around a dry patch on the substrate, as sketched in Figure 1. Cartesian coordinates  $Oxyz$  with the  $x$  axis down the line of greatest slope and the  $z$  axis normal to the substrate are adopted, with the substrate at  $z = 0$ . We denote the free surface profile of the film by  $z = h(x, y, t)$ , where  $t$  denotes time. We take the dry patch to be slender (varying much more slowly in the longitudinal ( $x$ ) direction than in the transverse ( $y$ ) direction), and we neglect surface-tension effects. Then with the familiar lubrication approximation, the velocity  $(u, v, w)$ , pressure  $p$  and thickness  $h$  satisfy the governing equations:

$$u_x + v_y + w_z = 0, \tag{1}$$

$$\mu u_{zz} + \rho g \sin \alpha = 0, \tag{2}$$

$$-p_y + \mu v_{zz} = 0, \tag{3}$$

$$-p_z - \rho g \cos \alpha = 0. \tag{4}$$

We integrate (1)–(4) subject to the boundary conditions of no slip and no penetration on the substrate  $z = 0$ :  $u = v = w = 0$ , and balances of normal and tangential stresses on the free surface  $z = h$ :  $p = p_a$ ,  $\mu u_z = \tau$ ,  $v_z = 0$  (where  $p_a$  denotes atmospheric pressure) to yield:

$$p = p_a + \rho g \cos \alpha (h - z), \tag{5}$$

$$u = \frac{\rho g \sin \alpha}{2\mu} (2h - z)z + \frac{\tau}{\mu} z, \tag{6}$$

$$v = -\frac{\rho g \cos \alpha}{2\mu} h_y (2h - z)z, \tag{7}$$

$$w = -\frac{\rho g \sin \alpha}{2\mu} h_x z^2 + \frac{\rho g \cos \alpha}{6\mu} (3h_y^2 + (3h - z)h_{yy})z^2. \tag{8}$$

We introduce local fluxes  $\bar{u} = \bar{u}(x, y, t)$  and  $\bar{v} = \bar{v}(x, y, t)$  given by:

$$\begin{aligned} \bar{u} &= \int_0^h u dz = \frac{\rho g \sin \alpha}{3\mu} h^3 + \frac{\tau}{2\mu} h^2, \\ \bar{v} &= \int_0^h v dz = -\frac{\rho g \cos \alpha}{3\mu} h^3 h_y, \end{aligned} \tag{9}$$

and hence the kinematic condition on  $z = h$ , which may be written in the form  $h_t + \bar{u}_x + \bar{v}_y = 0$ , yields the governing partial differential equation for  $h$ :

$$h_t = \frac{\rho g \cos \alpha}{3\mu} (h^3 h_y)_y - \frac{\rho g \sin \alpha}{3\mu} (h^3)_x - \frac{\tau}{2\mu} (h^2)_x. \tag{10}$$

Once  $h$  is determined from (10) the solution for  $p$ ,  $u$ ,  $v$  and  $w$  in (5)–(8) is known.

In the case of a film of constant uniform thickness  $h_\infty$  the solution takes the form  $p = p_\infty(z)$ ,  $u = u_\infty(z)$ ,  $v = v_\infty = 0$  and  $w = w_\infty = 0$ , where

$$\begin{aligned} p_\infty &= p_a + \rho g \cos \alpha (h_\infty - z), \\ u_\infty &= \frac{\rho g \sin \alpha}{2\mu} (2h_\infty - z)z + \frac{\tau}{\mu} z, \end{aligned} \tag{11}$$

representing steady unidirectional flow down the substrate, with depth-averaged velocity  $U\mathbf{i}$ , where

$$U = \frac{\rho g \sin \alpha}{3\mu} h_\infty^2 + \frac{\tau}{2\mu} h_\infty. \tag{12}$$

We are concerned with the unsteady flow around a dry patch in a film of thickness  $h_\infty$  at infinity (that is, in a

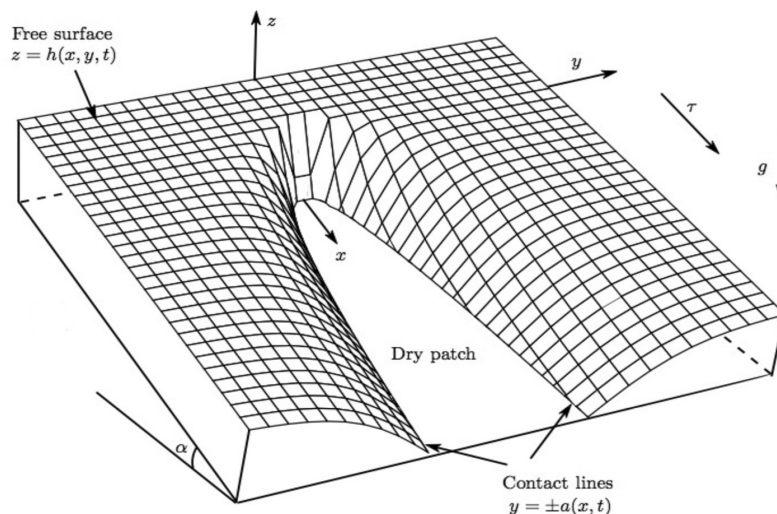


FIGURE 1. Sketch of a moving dry patch in a thin film

film that would be of uniform thickness  $h_\infty$  if the dry patch were absent). We shall restrict attention to dry patches that are symmetric about  $y = 0$  (so that  $h$  is even in  $y$ ) with (unknown) semi-width  $a = a(x, t)$ , so that the fluid occupies  $|y| \geq a$ , and  $h = 0$  at the contact lines  $y = \pm a$ . The zero-mass-flux condition at the contact lines  $y = \pm a$  is  $\bar{v} = \pm a_x \bar{u}$ , and from (9) we have  $\bar{u} = 0$  at  $y = \pm a$ ; therefore we have the contact-line conditions  $h = 0$  at  $y = \pm a$  and  $h^3 h_y \rightarrow 0$  as  $y \rightarrow \pm a$ .

Of particular interest is the case of flow on a substrate driven by surface shear with the down-slope component of gravity neglected, which is equivalent to setting  $\sin \alpha = 0$ . Hence (10) reduces to:

$$h_t = \frac{\rho g \cos \alpha}{3\mu} (h^3 h_y)_y - \frac{\tau}{2\mu} (h^2)_x. \tag{13}$$

The case of flow driven purely by gravity was considered by Yatim et al. (2012).

A SIMILARITY SOLUTION

We seek an unsteady travelling-wave similarity solution of (13) in the form:

$$h = h_\infty F(\eta), \eta = \frac{y}{[\ell(x-ct)]^{1/2}} \text{ if } \ell(x-ct) \geq 0, \\ h = h_\infty \text{ if } \ell(x-ct) < 0, \tag{14}$$

where  $c\mathbf{i}$  (with  $c > 0$ ) is the velocity of the dry patch down the substrate, the dimensionless function  $F = F(\eta) (\geq 0)$  of the dimensionless similarity variable  $\eta$  is to be determined, and the constant  $\ell$  is to be specified. The dry patch lies in the region where  $\ell(x-ct) \geq 0$  and the fluid in the region where  $\ell(x-ct) < 0$  (ahead of or behind the dry patch) is of uniform thickness  $h = h_\infty$ ; at  $x = ct$  the thickness  $h$  and its derivative  $h_y$  are continuous (so that  $u, v$  and  $p$  are continuous there), except at the singular point  $x = ct, y = 0$ , at which the free surface is normal to the substrate, occupying  $0 \leq z \leq h_\infty$ . With (14), (13) reduces to an ordinary differential equation for  $F(\eta)$ , namely:

$$(F^3 F')' + \frac{3\tau \ell}{4\rho g \cos \alpha h_\infty^2} \eta \left( F^2 - \frac{c}{U} F \right)' = 0, \tag{15}$$

where a dash denotes differentiation with respect to  $\eta$  and from (12),  $U = \tau h_\infty / 2\mu (> 0)$  is the depth-averaged velocity of the flow (11) in this case. Without loss of generality we now write:

$$\ell = \frac{4\rho g \cos \alpha h_\infty^2}{3\tau}. \tag{16}$$

We denote the (unknown) position where  $F = 0$  by  $\eta = \eta_0$  (corresponding to the contact-line position  $y = a$ ), so that the fluid lies in  $|\eta| \geq \eta_0$  and

$$a = \sqrt{\ell(x-ct)} \eta_0, \frac{y}{a} = \frac{\eta}{\eta_0}, \tag{17}$$

showing that the dry patch has a parabolic shape. The solutions obtained in this study could represent two physical cases, namely the sessile case and the pendent case. In the sessile case ( $\cos \alpha > 0$ , so that  $\ell > 0$ ) the dry patch occupies  $x \geq ct$ , with semi-width  $a = \sqrt{\ell(x-ct)} \eta_0$  (widening with increasing  $x$ ), whereas in the pendent case ( $\cos \alpha < 0$ , so that  $\ell < 0$ ) it occupies  $x \leq ct$ , with semi-width  $a = \sqrt{|\ell|(ct-x)} \eta_0$  (narrowing with increasing  $x$ ).

We now non-dimensionalise and re-scale variables according to  $x = Xx^*, y = \sqrt{|\ell|} Xy^*, z = h_\infty z^*, t = (X/U)t^*, h = h_\infty h^*, a = \sqrt{|\ell|} Xa^*, c = Uc^*$ , where  $X (>> h_\infty)$  is a length scale in the  $x$  direction, which we may choose arbitrarily. Then with stars dropped for clarity the solution (14) takes the slightly simpler form:

$$h = F(\eta), y = \sqrt{Sg(x-ct)} \eta, a = \sqrt{Sg(x-ct)} \eta_0, \tag{18}$$

(where we have defined  $Sg = \text{sgn}(\cos \alpha)$ ), with  $F$  now satisfying:

$$(F^3 F')' + \eta (F^2 - cF)' = 0, \tag{19}$$

to be integrated subject to the contact line conditions:

$$F = 0 \text{ at } \eta = \eta_0, F^3 F' \rightarrow 0 \text{ as } \eta \rightarrow \eta_0, \tag{20}$$

and the far-field condition:

$$F \rightarrow 1 \text{ as } \eta \rightarrow \infty. \tag{21}$$

Near the contact line  $\eta = \eta_0$  the behaviour of  $F$  is given by

$$F \sim [3c\eta_0(\eta - \eta_0)]^{1/3} \tag{22}$$

in the limit  $\eta \rightarrow \eta_0^+$ , provided that  $c > 0$ . Also (22) shows that the fluid film has infinite slope at the contact line  $\eta = \eta_0$  and so the lubrication approximation fails there. In the limit  $\eta \rightarrow \infty$  the behaviour of  $F$  is found to be:

$$F - 1 \propto \frac{1}{\eta} \exp\left(-\frac{2-c}{2} \eta^2\right), \tag{23}$$

provided that  $c < 2$ . Equation (23) shows that the transverse profile of the fluid film approaches the uniform far-field value in (21) monotonically.

Conditions for the dry patch to be thin and slender are that the length scales in the  $x, y$  and  $z$  directions, namely  $X, \sqrt{|\ell|} X$  and  $h_\infty$ , satisfy  $h_\infty \ll \sqrt{|\ell|} X \ll X$ , so that

$$X \gg \frac{\tau}{\rho g |\cos \alpha|}, X \gg \frac{\rho g |\cos \alpha| h_\infty^2}{\tau}, \tag{24}$$

respectively, showing that  $X$  must be sufficiently large and that  $\alpha$  cannot be close to  $\pi/2$ .

NUMERICAL SOLUTION FOR  $F(\eta)$

Since a closed-form solution of (19) is not available, we solved it numerically for  $F$ . We did this using a shooting method, by shooting from a chosen value of the contact-line position  $\eta = \eta_0$ , with a chosen value of  $c$ . The solution  $F$  was monitored to see if it satisfied (21) to within a prescribed tolerance; if not then the value of  $c$  was changed and the calculation repeated until a solution satisfying (21) was found. In fact, the numerical computation cannot be started at  $\eta = \eta_0$  (because of the singular slope there, given by (22)), so instead it was started from a position  $\eta = \eta_0 + \delta$ , where  $\delta (> 0)$  is small; thus we solved (19) subject to the approximated boundary conditions:

$$F(\eta_0 + \delta) = (3c\eta_0\delta)^{\frac{1}{3}}, \quad F'(\eta_0 + \delta) = \left(\frac{c\eta_0}{9\delta^2}\right)^{\frac{1}{3}}, \quad (25)$$

obtained from (22).

Figure 2 shows a plot of  $c$  as a function of  $\eta_0$  obtained in this way. As Figure 2 shows,  $c$  is a single-valued function of  $\eta_0$ , but behaves non-monotonically. It is found that  $c$  decreases from its value  $c = c_0 \approx 1.5424$  when  $\eta = 0$  to a (local) minimum value  $c = c_{min} \approx 1.5421$  when  $\eta_0 \approx 0.0040$ , then increases to a (global) maximum value  $c = c_{max} \approx 1.5503$  when  $\eta_0 \approx 0.0470$  and then decreases monotonically towards the value  $c = 1$  as  $\eta_0 \rightarrow \infty$ . Thus the scaled speed of the dry patch satisfies  $1 < c \leq c_{max}$  for any value of  $\eta_0$ , more restrictive than the condition  $0 < c < 2$  obtained above. Also there can be up to three different dry patches that travel at a given speed  $c$  in this interval; specifically for a given value of  $c$ , there is one corresponding value of  $\eta_0$  if either  $c = c_{max}$  or  $1 < c < c_{min}$ , two if either  $c_0 < c < c_{max}$  or  $c = c_{min}$ , three if  $c_{min} < c < c_0$  and none if either  $c > c_{max}$  or  $c \leq 1$ . The results also demonstrate that as the dry patch widens its speed eventually decreases.

In the limit of a narrow dry patch,  $\eta_0 \rightarrow 0$ , we write  $\eta$ ,  $F$  and  $c$  in the form  $\eta = \eta_0 + \hat{\eta}$ ,  $F = \hat{F}(\hat{\eta})$ ,  $c = c_0$ ; then at leading order (19) gives:

$$(\hat{F}^3 \hat{F}') + \hat{\eta}(\hat{F}^2 - c_0 \hat{F})' = 0, \quad (26)$$

and (20) and (21) give the conditions:

$$\hat{F} = 0 \text{ at } \hat{\eta} = 0, \quad \hat{F}^3 \hat{F}' \rightarrow 0 \text{ as } \hat{\eta} \rightarrow 0, \quad \hat{F} \rightarrow 1 \text{ as } \hat{\eta} \rightarrow \infty. \quad (27)$$

At leading order in the limit  $\hat{\eta} \rightarrow 0$  the solution of (26) and (27) for  $\hat{F}$  has the asymptotic form:

$$\hat{F} \sim \left(\frac{3}{5} c_0 \hat{\eta}^2\right)^{\frac{1}{3}}. \quad (28)$$

We solved (26) for  $\hat{F}$  numerically using a shooting method similar to that described above, subject to approximated boundary conditions obtained from (28), namely:

$$\hat{F}(\delta) = \left(\frac{3}{5} c_0 \delta^2\right)^{\frac{1}{3}}, \quad \hat{F}'(\delta) = \frac{2}{3} \left(\frac{3c_0}{5\delta}\right)^{\frac{1}{3}}, \quad (29)$$

where  $0 < \delta \ll 1$ . From this numerical solution it is found that  $c_0 \approx 1.5424$ , confirming the value obtained earlier.

In the limit of a wide dry patch,  $\tilde{\eta} \rightarrow \infty$ , we write  $\eta$ ,  $F$  and  $c$  in the form  $\eta = \eta_0 + \tilde{\eta}/\eta_0$ ,  $F = \tilde{F}(\tilde{\eta})$ ,  $c = c_\infty$ ; then at leading order (19) reduces to:

$$(\tilde{F}^3 \tilde{F}') + (\tilde{F}^2 - c_\infty \tilde{F})' = 0, \quad (30)$$

which is readily solved subject to the conditions  $\tilde{F} = 0$  at  $\tilde{\eta} = 0$ ,  $\tilde{F}^3 \tilde{F}' \rightarrow 0$  as  $\tilde{\eta} \rightarrow 0$ ,  $\tilde{F} \rightarrow 1$  as  $\tilde{\eta} \rightarrow \infty$  to give the implicit solution:

$$\tilde{\eta} = -\tilde{F} - \frac{\tilde{F}^2}{2} - \log(1 - \tilde{F}), \quad c_\infty = 1. \quad (31)$$

The asymptotic value  $c = c_\infty = 1$  is included in Figure 2 as a dashed line.

Figure 3 shows examples of cross-sectional profiles  $F(\eta)$  for various values of  $\eta_0$ . In particular, the cross-

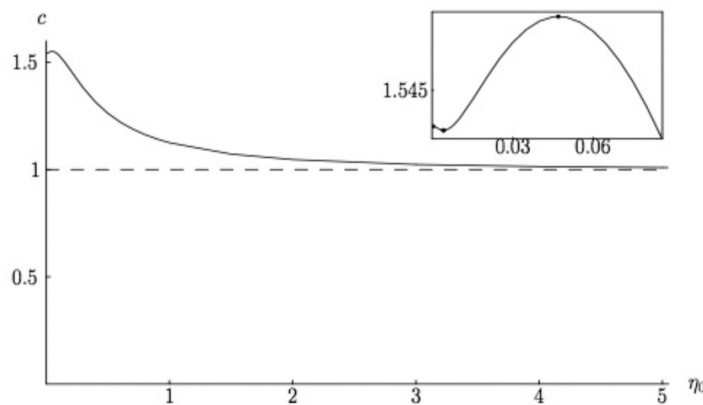


FIGURE 2. Plot of  $c$  as a function of  $\eta_0$ , together with the asymptotic value  $c = c_\infty = 1$  in the limit  $\eta_0 \rightarrow \infty$  (shown as a dashed line). The inset shows an enlargement of the behaviour near  $\eta_0 = 0$ ; the point  $c = c_0 \approx 1.5424$  at  $\eta_0 = 0$  is shown as a dot, as are the minimum  $c = c_{min} \approx 1.5421$  at  $\eta_0 \approx 0.0040$  and the maximum  $c = c_{max} \approx 1.5503$  at  $\eta_0 \approx 0.0470$

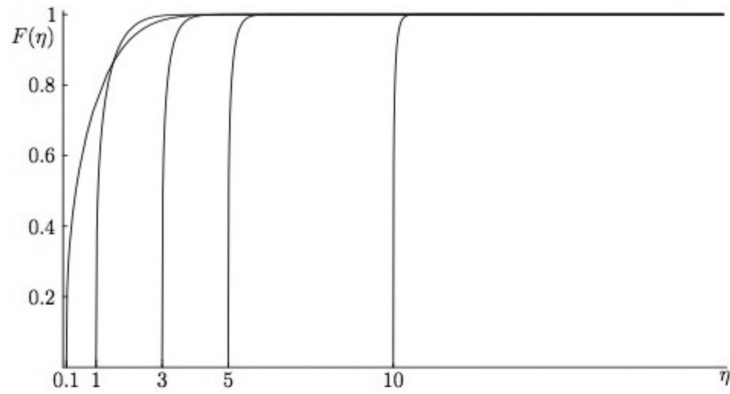


FIGURE 3. Cross-sectional profiles  $F(\eta)$  for  $\eta_0 = 0.1, 1, 3, 5$  and  $10$

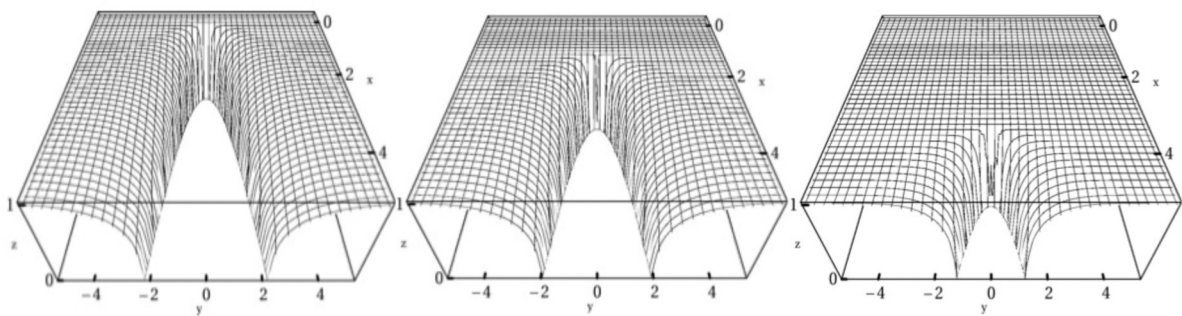


FIGURE 4. Three-dimensional plots of the free-surface profiles  $z = h$  in a sessile case with  $\eta_0 = 1$  at times  $t = 0, 3$  and  $5$

sectional profiles  $F$  increase monotonically with  $\eta$ , from  $F = 0$  at  $\eta = \eta_0$  to  $F = 1$  as  $\eta \rightarrow \infty$ .

Figure 4 shows three-dimensional plots of the free-surface profiles  $z = h$  in a sessile case with  $\eta_0 = 1$  predicted by the similarity solution (14) at times  $t = 0, 3$  and  $5$ . Noticeably, the dry patch becomes narrower and eventually will be swept away as time increases.

CONCLUSION

We have obtained unsteady travelling-wave similarity solutions of the form (14) for an infinitely wide thin film of Newtonian fluid of uniform thickness  $h_\infty$  flowing around a symmetric slender dry patch moving at constant velocity  $ci$  on an inclined planar substrate, the flow being driven by a constant shear stress at the free surface. The solutions may be interpreted as representing either a sessile case ( $0 < \alpha < \pi/2$ ) or a pendent case ( $\pi/2 < \alpha < \pi$ ). The dry patch has a parabolic shape, its scaled semi-width  $a$  varying like  $|x - ct|^{1/2}$ , where  $1 < c \leq c_{max} \approx 1.5503$ , and the film thickness increases monotonically away from the dry patch.

The parameter  $\eta_0$  is not determined as part of the solution, so that (14) represents a one-parameter family of solutions; some additional criterion would be required to determine  $\eta_0$ . The solutions obtained are valid for any value of  $h_\infty$ , showing that for these solutions there is no critical thickness or critical flux below which a dry patch

can be stationary but above which it is swept away by the bulk flow.

ACKNOWLEDGEMENT

The first author (Y.M. Yatim) wishes to thank the Universiti Sains Malaysia for financial support via an Incentive Grant.

REFERENCES

Hartley, D.E. & Murgatroyd, W. 1964. Criteria for the break-up of thin liquid layers flowing isothermally over solid surfaces. *Int. J. Heat Mass Transfer* 7: 1003-1015.  
 Murgatroyd, W. 1965. The role of shear and form forces in the stability of a dry patch in two-phase film flow. *Int. J. Heat Mass Transfer* 8: 297-301.  
 Podgorski, T., Flesselles, J.-M. & Limat, L. 1999. Dry arches within flowing films. *Phys. Fluids* 11: 845-852.  
 Podgorski, T., Flesselles, J.-M. & Limat, L. 2001. Curvature of a dry patch boundary in a flowing film. *C. R. Acad. Sci., Ser IV* 2: 1361-1367.  
 Ponter, A.B., Davies, G.A., Ross, T.K. & Thornley, P.G. 1967. The influence of mass transfer on liquid film breakdown. *Int. J. Heat Mass Transfer* 10: 349-359.  
 Rio, E., Daerr, A. & Limat, L. 2004. Probing with a laser sheet the contact angle distribution along a contact line. *J. Colloid Interface Sci.* 269: 164-170.  
 Rio, E. & Limat, L. 2006. Wetting hysteresis of a dry patch left inside a flowing film. *Phys. Fluids* 18: 032102-1–032102-8.

- Sćbilleau, J., Lebon, L. & Limat, L. 2009. Stability of a dry patch in a viscous flowing film. *Eur. Phys. J. Special Topics* 166: 139-142.
- Wilson, S.K., Duffy, B.R. & Davis, S.H. 2001. On a slender dry patch in a liquid film draining under gravity down an inclined plane. *Eur. J. Appl. Math.* 12: 233-252.
- Yatim, Y.M., Duffy, B.R. & Wilson, S.K. 2012. Travelling-wave similarity solutions for an unsteady gravity-driven dry patch. In *Progress in Industrial Mathematics at ECMI 2010*. Heidelberg: Springer-Verlag. pp. 441-447.

Yazariah M. Yatim\*  
School of Mathematical Sciences  
Universiti Sains Malaysia  
11800 Penang  
Malaysia

Brian R. Duffy & Stephen K. Wilson  
Department of Mathematics and Statistics  
University of Strathclyde  
G1 1XH Glasgow  
United Kingdom

\*Corresponding author; email: yazariahmy@usm.my

Received: 1 February 2012  
Accepted: 16 January 2013